We are IntechOpen,
the world's leading publisher of Open Access books
Built by scientists, for scientists

6,900
Open access books available

186,000
International authors and editors

200M
Downloads

Our authors are among the

154
Countries delivered to

TOP 1%
most cited scientists

12.2%
Contributors from top 500 universities

Interested in publishing with us?
Contact book.department@intechopen.com

Numbers displayed above are based on latest data collected.
For more information visit www.intechopen.com

Quantum Signal over Optical Fiber

Nor Roshidah Yusof, Norshamsuri Ali,
Syed Alwee Aljunid Syed Junid, Mohd Rashidi Che Beson
and Rosdisham Endut

Abstract

This chapter aims to address the quantum signal role and properties in optical fiber application mainly in quantum communication. It covers the general discussion on quantum bits and optical waveguiding properties. The highlight of this chapter lies in the discussion of the quantum fictitious force of anti-centrifugal force which was first reported in 2001. Under this condition, the free particle experience an attractive potential towards the rotating center of a bent waveguide structure. A lot of theoretical work has been carried out to observe this quantum phenomenon. However, no intensive experimental work has been carried out to date. With the advancement of nano-fabrication technology and quantum experimental, it provides a bright potential to observe these phenomena. Thus, we proposed a promising material of Lithium Niobate on Insulator to serve as a waveguiding platform to study this quantum effect experimentally. The discussion is extended to perceive the relation between Schrodinger and Helmholtz's equation corresponding to this effect.

Keywords: quantum anti-centrifugal force, waveguide, rib waveguide, LNOI, spatial mode

1. Introduction

Optical fiber is known as one of the passive devices that serve as the transmission medium in optical communications. This cylindrical-shaped dielectric waveguide consists of the higher refractive index inner core surrounded with slightly lower index cladding which operates based on total internal reflection phenomena. To date, the advancement in optical fiber technology led to the development of new fiber designs and components to establish multiple co-existing data channels based on light propagation over distinct transverse optical modes [1]. Apart from that, there have been tremendous research and developments in quantum information processing since Richard Feynman's seminal talk on the future of quantum computing 40 years ago. These developments have been motivated by the higher demand for higher transmission bandwidth in telecommunication infrastructure. Thus, optical fiber has played its main role in the success of this technology mainly due to its high transparency and high-bandwidth support [2]. Thus, the discussion of this chapter covers the general idea of quantum bits which has become the backbone in quantum information.

Apart from that, it is found that the bending of optical waveguide has led to the signal distortion which increase the propagation losses. For the pass few years, researcher put an extra effort to observe this phenomena which is known an quantum anti-centrifugal force from a quantum physics point of view.

Therefore, the aim of this chapter lies on the discussion of poorly reviewed quantum anti-centrifugal force. Furthermore, we perceive the correlation of modern interpretation of Schrodinger equation with the classical Helmholtz equation correspond to this quantum fictitious force. The observation of this effect is extended into the real application of Lithium Niobate on Insulator rib waveguide as it found to be an extensive platfrom towards the development of quantum information technology.

2. Optical field propagation

The optical waveguide structure consists of high refractive index core, surrounded by slightly lower refractive index. It operates based on total internal reflection phenomena which allow the electromagnetic wave guiding towards core. The electromagnetic plane waves propagation in homogeneous and isotropic media such as glass and diamond are governed by Maxwell's equation:

$$\nabla \times E + \mu \frac{\partial H}{\partial t} = 0 \tag{1}$$

$$\nabla \times H - \varepsilon \frac{\partial E}{\partial t} = 0 \tag{2}$$

The permittivity tensor, ε, and permeability tensor, μ is uniform. Both of Eqs. (1) and (2) are satisfied by the following plane wave solution:

$$\Psi = A e^{-i(\omega t - k.r)} \tag{3}$$

where A and ω denotes an amplitude and angular frequency with the wavevector, $|k| = \omega \sqrt{\mu \varepsilon}$.

However, for the anisotropic media such as Lithium niobate, calcite, and quartz, both ε and μ are directional dependent [3]. The permittivity tensor is derived by the following matrix expression:

$$\varepsilon = \varepsilon_o \begin{bmatrix} n_x^2 & 0 & 0 \\ 0 & n_y^2 & 0 \\ 0 & 0 & n_z^2 \end{bmatrix} = \begin{bmatrix} \varepsilon_x & 0 & 0 \\ 0 & \varepsilon_y & 0 \\ 0 & 0 & \varepsilon_z \end{bmatrix} \tag{4}$$

where n_x, n_y and n_z are the principal indices of refraction whereas (x, y, z) denotes the principal axis of the crystal. Generally, the anisotropic media can be divided into uniaxial and biaxial crystal. In uniaxial medium, the refractive index corresponds to two equal principle elements i.e. $n_o^2 = \varepsilon_x/\varepsilon_o = \varepsilon_y/\varepsilon_o$ is defined as an ordinary index, n_o whereas the other index for the remaining principle ($n_{eo}^2 = \varepsilon_z/\varepsilon_o$) is known extraordinary index.

The optical mode across the waveguiding area is derived from the abovementioned Maxwell's equation and Helmholtz propagation equation with a specific boundary condition. From this, it can show the deformation of spatial modes and optical loss in optical fiber [4–6]. The Helmholtz problem can be solved analytically when it is separable concerning its variables. However, this separability

does not hold for all coordinate systems [7]. Therefore, the need to choose for a suitable coordinate system and boundary conditions are crucially needed prior to solve the eigenmode problem analytically.

Another limitation with regards to geometrical structure are sharp corners, e.g. a rectangular one, which requires approximations such as the assumption of strong field confinement in the waveguide [8, 9]. In cylindrical coordinates $(r; \varphi)$ the Helmholtz equation takes the form of

$$\left(\frac{1}{r}\frac{\partial}{\partial r} + \frac{\partial^2}{\partial r^2} + \frac{1}{r^2}\frac{\partial^2}{\partial \varphi^2} + k_0^2 n^2(r)\right)\Psi(\mathrm{r}, \varphi) = 0 \tag{5}$$

where $n(r)$ denotes the refractive index and $\Psi(r, \varphi) = \psi(r)\Phi(\varphi)$. $\psi(r)$ represents the bending mode profile.

At the bending area, it shows a higher tendency to produce radiation loss compared to straight waveguide due to the variance of phase front velocity correspond to the speed of light. These modes are strongly guided in the area with the highest refractive index. Thus, it will shift towards the outer surface of the bent waveguide. At the transition from straight to bent waveguide mode adaptation, losses will occur. Unfortunately, these losses are exponentially increased as we reduced the radii of curvature, which led to major drawbacks in developing nano-sized optical waveguiding devices.

3. Quantum anti-centrifugal force

Among quantum fictitious forces, the quantum anticentrifugal force which appears in the cylindrical symmetry system belongs to the most fascinating. This quantum phenomenon was first reported by [10] where he predicted that a free particle of vanishing angular momentum, $m = 0$ experiences an attractive potential towards the rotating centre rather than repulsive. The 2-dimension time-independent Schrödinger equation of the free particle of mass, M and energy, E along the polar coordinates r and φ is given by

$$\left\{\frac{d^2}{dr^2} + \frac{2M}{\hbar^2}[E - V_m(r)]\right\}u_m(r) = 0 \tag{6}$$

$$V_m(r) = \frac{\hbar^2}{2M}\frac{m^2 - 1/4}{r^2} \tag{7}$$

where $u_m(r)$ and $V_m(r)$ is a radial wave function and effective potential, respectively. This potential describes the existence of repulsive or attractive force on the free particle which is proportional to the value of m^2. Under the non-vanishing angular momentum $(m \neq 0)$ condition, it tends to repulse far from the rotating center thus, create the centrifugal force. On contrary, at zero angular momentum, its binding potential towards the rotating center become stronger and contribute to the arising of quantum anti-centrifugal potential, V_Q which is given by

$$V_Q \equiv V_0(r) = -\frac{\hbar^2}{2M}\frac{1}{4r^2} \tag{8}$$

The force corresponding to V_Q cause a ring-shaped wave packet to spread in an asymmetric form where it spreads faster towards the origin. Consequently, the particle is localized on a band-shaped domain around the origin. On contrary,

Cirone claimed that this potential force has not existed in 3-dimensional space. However, in 2010, Dandoloff proves that this counterintuitive potential existed in 3-dimensional space on wormhole geometry [11].

In 2011, he reported his finding on quantum anti-centrifugal potential dependences over the radius of the bent rectangular waveguide as depicted in **Figure 1** [12, 13]. Based on the following line element expression, the Schrödinger equation of this Cartesian coordinate can be derived as Eq. (10).

$$dr^2 = d\xi^2 + dz^2 + (1 - \kappa\xi)^2 ds^2 \qquad (9)$$

$$\Delta\Psi = \frac{\partial^2\Psi}{\partial z^2} + \frac{\delta^2\Psi}{\delta\xi^2} - \frac{\kappa}{(1 - \kappa\xi)}\frac{\delta\Psi}{\delta\xi} + \frac{1}{(1 - \kappa\xi)^2}\frac{\delta^2\Psi}{\delta\xi^2} \qquad (10)$$

where $\xi \in \left[-\frac{a}{2}, \frac{a}{2}\right]$, $\kappa = \frac{1}{R}$, $C = C(a, R)$ and $\Psi = \frac{1}{\sqrt{C}}\frac{\Phi}{1 - \kappa\xi}$.

The general time-independent Schrödinger equation of $\frac{i\hbar^2}{2M}\Delta\Psi = E\Psi$ is then can be expressed in (ξ, s, z) coordinate system as:

$$E\frac{\Phi}{(1 - \kappa\xi)^{\frac{1}{2}}} = \frac{i\hbar^2}{2M}\left[\frac{1}{(1 - \kappa\xi)^{\frac{1}{2}}}\frac{\delta^2\Phi}{\delta\xi^2} + \frac{k^2}{4}\frac{\Phi}{(1 - \kappa\xi)^{\frac{5}{2}}} + \frac{\partial^2\Phi}{\partial z^2} + \frac{1}{(1 - \kappa\xi)^2}\frac{\delta^2\Phi}{\delta s^2}\right] \qquad (11)$$
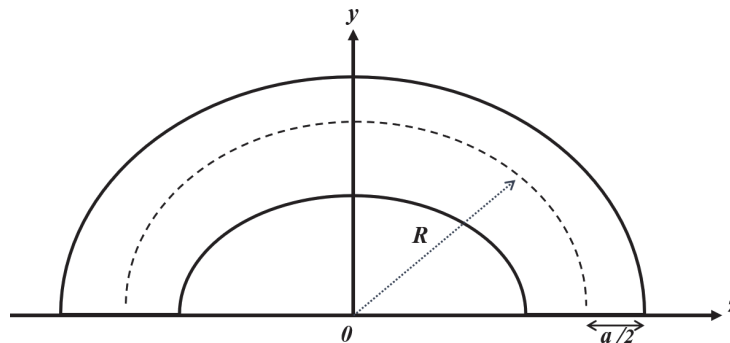
Compared to Eq. (8), Dandoloff proposed the Bohm potential, Q corresponding to the bent waveguide which is given by

$$Q = -\frac{\hbar^2}{2M}\frac{\Delta R}{R} \qquad (12)$$

where R is the radius of the waveguide. This force was assumed to affect the quantum motion on a bent waveguide. However, he found that this effect has a very weak contribution to the overall potential. Thus, the quantum anti-centrifugal potential is then derived as:

$$-\frac{\hbar^2}{2M}\frac{dV_{eff}}{d\xi}\bigg|_{\xi=0} = \frac{\hbar^2}{2M}\frac{\kappa^3}{2} = \frac{\hbar^2}{2M}\frac{1}{2R^3} \qquad (13)$$

It is found that at zero angular momentum (m = 0), the anti-centrifugal reciprocally dependence on R³. Dandaloff also concluded the similarity of the stationary Schrödinger equation and Helmholtz equation for the TE modes in a waveguide structure. Subsequently, the interference pattern in the quantum medium should have the same pattern as an electromagnetic wave in a bent waveguide.

Figure 1.
Semi-circular shaped bent waveguide on Cartesian coordinates, (x,y,z).

In 2015, Victor published another finding on quantum anti-centrifugal potential by introducing half-geodesic coordinates where the curvature with constant radius corresponds to the concentric circles at $r = 0$ [7]. Its 2D Laplacian function is expressed as:

$$\Delta\psi = \frac{1}{h}\left[\frac{\partial h}{\partial r}\left(h\frac{\partial h}{\partial r}\right) + \frac{\partial}{\partial\phi}\left(\frac{1}{h}\frac{\partial h}{\partial\phi}\right)\right]\psi \tag{14}$$

In this work, an intrinsic Gaussian curvature of the surface, $K = -h^{-1}\partial_r^2 h$ and the geodesic curvature of the geodesically parallel coordinates lines $k_g = -h^{-1}\partial_r h$ has been introduced. Thus, the effective potential, V may be written as follows:

$$V = \frac{\hbar^2}{2M}\left(\frac{m^2}{h^2} - \frac{1}{4}k_g^2 - \frac{1}{2K}\right) \tag{15}$$

Within the limit of $\frac{\omega r}{c} \ll 1$, $k_g = \frac{1}{r^2} + 2\frac{\omega^2}{c^2}$ and $K = -3\frac{\omega^2}{c^2}$, Eq. (14) can be expressed as:

$$V = -\frac{\hbar^2}{2M}\left(\frac{m^2 - \frac{1}{4}}{r^2} - \left(m^2 - 1\right)\frac{\omega^2}{c^2}\right) \tag{16}$$

Eq. (15) describes the anti-centrifugal potential in a 2D plane at any surface which can be covered globally with a geodesically parallel coordinate system. At $K > 0$ (i.e elliptical), the curvature weakens the anti-centrifugal potential whereas at $K < 0$ (i.e catenoid), its potential enhanced. Recently, Dandoloff has included the quantum geometric potential (QGP) which commonly occurs at the surface of the structure, using a very high sandwich potential around the surface. The total effective potential is given by:

$$V = \frac{\hbar^2}{2M}\left(\frac{m^2}{h^2} - \frac{1}{4}k_g^2 - \frac{1}{2K}\right) \tag{17}$$

From this research, Dandoloff addressed his new finding on the total quantum effective potential which appears to be the nonlinear sigma model plus positive terms instead of the negative signage. Even though the exact number of states cannot be defined by using this Topologically Stable States, but it provides the centrifugal states additional legitimacy [14, 15].

4. Schrödinger vs. Helmholtz equation towards the measurement of quantum anti-centrifugal force

As of today, the investigation of the quantum anti-centrifugal potential was investigated purely theoretical correspond to the Schrödinger equation. However, the advancement of the nano-fabrication and quantum photonics technology since last decides has brought the impossible into reality. It has become a thriving field of research in promoting both fundamental studies of quantum phenomena and a wider range of disruptive quantum technologies. The well-developed quantum experimental setting such as the phase retrieval algorithm and single-photon detection techniques has brought the experimental on quantum anti-centrifugal potential into reality. Recently, a lot of studies on spatial mode deformation and losses in optical fiber in various geometrical structure has been carried out to observe the
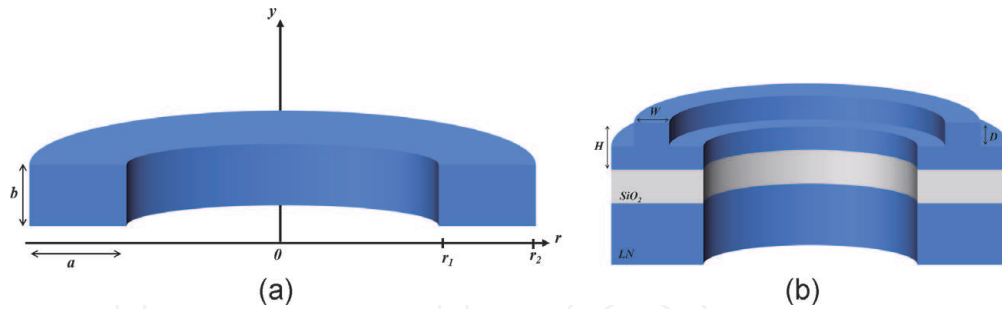
similar quantum effect by using the Helmholtz equation with a suitable boundary condition.
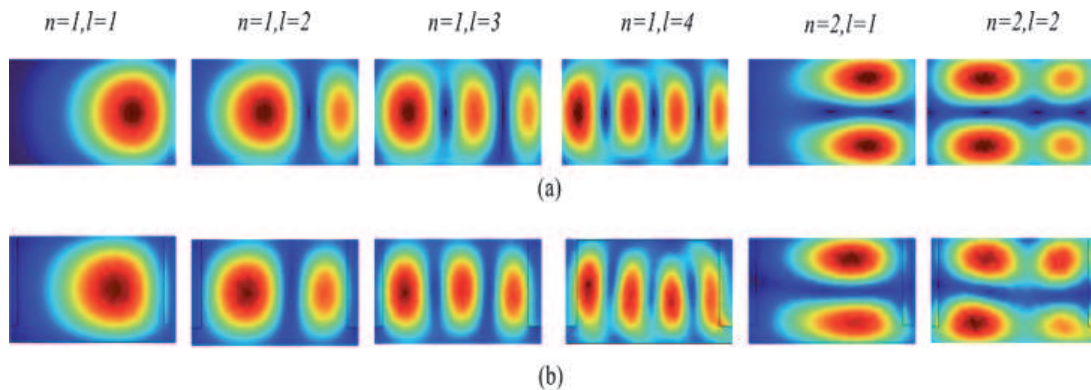
Recently, the deformation of eigenmode in the semi-circular toroidal waveguide is reported in [17] as depicted in **Figure 2(a)** by using the finite element method. The operating wavelength and refractive index of both waveguides, n_w and surrounding, n_s was set at 800 nm and 2.3 and 1.0, respectively. The mode average radial position was introduced in this simulation work in order to analyze the direction of mode. The bending radius was set at 1 μm. On top of that, the analysis was extended to a realistic structure and promising material in quantum photonic technology, Lithium Niobate on insulator (LNOI) rib waveguide [16]. Lithium Niobate (LN) is has a strong nonlinear electro-optical property which transparent over a broad spectrum spanning from visible to mid-infrared region (350 nm to 5200 nm).

Figure 2(b) depicted the rib structure which consists of 500 um thick LN substrate, 2 μm thick SiO_2 which acts as a buffer layer, and a 600 nm thin film LN. The thin film LN is etched to form the higher confinement core with height, D, and width, W of 500 nm and 1000 nm, respectively. This simulation was performed in an axial-symmetric profile at a second harmonic wavelength of 775 nm.

Based on **Figure 3(a)**, the spatial mode distorted and shifted towards the outer wall of the bent waveguide. As the mode propagates across the waveguide, it is strongly guided towards the area with a higher refractive index that leads to the mode shifting towards the outer rim of the bent waveguide. The maximum higher-order propagating mode of (2,2) was obtained with the higher intensity are found to be closer towards the inner wall of the waveguide. The propagating mode must fulfill this condition: $n_s < n_{eff} < n_w$ where n_{eff} denotes the effective refractive index. This value describes the propagation characteristic of the mode which proportional to propagation constant, β but reciprocal to wavenumber, κ_o. The maximum value

Figure 2.
(a) Toroidal waveguide with a width of core, $a = r_2 - r_1 = 1$ μm and height, $b = 0.5$ μm where $r_1 = 0.5$ μm and $r_2 = 1.5$ μm. (b) LNOI rib waveguide with the thickness of the slab, $h = H - D$ [17].

Figure 3.
Mode profile of bent waveguide in (a) toroidal and (b) LNOI rib structure [17].

of n_{eff} contribute to the eigenmode (fundamental) solution of Maxwell's equation. However, if the condition is not met ($n_{eff} < n_s$), the confined mode is degenerated and produced the radiating mode which contributes to the increment of propagation losses. Fortunately, the mode profile of the LNOI rib waveguide shows a prominent similarity with the toroidal waveguide structure despite the radius variation as depicted in **Figure 3(b)**. This output shows a strong consistency with the analytical solution in [17]. However, the slight asymmetric of the mode profile is led by the natural consequences of the symmetry breaking due to the presence of the oxide layer.

The aim of this chapter is to extend the above analysis by considering the variation of a radius on the rib waveguide prior to observe the deformation pattern of the mode profile within the bending area. Thus, the bending radius is set from 5 to 90 μm at a fixed width of the core value of 1 μm. From **Table 1**, it shows that the average radial position reduced as we c, which is inline with the finding in [17]. Consequently, the number of higher order mode increased as we increase the bending radius. However, at higher bending radius, the mode profile shows the symmetrical pattern compared to lower bending radius which tend to produce the asymmetric profile towards the outer surface of the waveguide.

Based on **Table 2**, the effective refractive index value decreased which reflect the decrement of propagation constant value. Simultaneously, the bending loss is increase drastically as the bending radius increase. The value is contributed by the summation of radiation, absorption, and scattering losses. However, it is mainly contributed by the scattering losses which occur due to the spatial fluctuations of the refractive index or the sidewalls roughness of the waveguide and radiation loss due to the imperfect mode guiding across the waveguide (**Table 2**) [18].

Mode number	Average radial position, $r_{av}>$ (μm)											
	R = 5 μm		R = 10 μm		R = 30 μm		R = 50 μm		R = 70 μm		R = 90 μm	
	$l = 1$	$l = 2$	$l = 1$	$l = 2$	$l = 1$	$l = 2$	$l = 1$	$l = 2$	$l = 1$	$l = 2$	$l = 1$	$l = 2$
$n = 1$	1.199	1.3237	1.133	1.126	1.051	1.047	1.031	1.022	1.023	1.019	1.018	1.016
$n = 2$	1.014	—	0.977	0.982	0.987	1.00	0.988	1.102	0.997	1.003	0.995	1.002
$n = 3$	1.016	—	0.972	—	0.981	—	0.997	—	0.991	—	0.998	—
$n = 4$	—	—	0.900	—	0.995	—	0.996	—	0.980	—	0.900	—

Table 1.
The average radial position of LNOI rib waveguide for various bent radius.

Mode number	Effective refractive index, n_{eff}											
	R = 5 μm		R = 10 μm		R = 30 μm		R = 50 μm		R = 70 μm		R = 90 μm	
	$l = 1$	$l = 2$	$l = 1$	$l = 2$	$l = 1$	$l = 2$	$l = 1$	$l = 2$	$l = 1$	$l = 2$	$l = 1$	$l = 2$
$n = 1$	2.452	2.1574	2.331	2.125	2.223	2.022	2.207	2.012	2.201	2.000	2.197	1.997
$n = 2$	2.271	—	2.2087	2.0014	2.123	1.8542	2.096	1.842	2.090	1.837	2.087	1.834
$n = 3$	2.101	—	2.0603	2.0603	1.962	—	1.950	—	1.945	—	1.942	—
$n = 4$	—	—	1.8357	1.748	—	1.737	—	1.732	—	1.729	—

Table 2.
The effective refractive index of LNOI rib waveguide for various bent radius.

5. Conclusion

In summary, we have developed a numerical model solution based on the Helmholtz wave equation by using finite element method. The mode profiles of the numerical solution provide the information of optical signals in optical fiber. Thus we are shown the effect Quantum Anti-centrifugal force has a similar phenomenon as in the Helmholtz wave equation analytically. Note that, this is a consequence of the form of the Helmholtz equation which in this case is mathematically identical to the Schrödinger equation. Thus, the setups proposed in this work may provide a classical platform to test quantum phenomena in optical fiber. The development a numerical model of the bent structure for both toroidal and LNOI rib waveguide will serve as the best platform to conduct the fundamental investigation of this quantum fictitious force mainly in the classical platform. It allows one to predict the spatial mode number and profile accurately. From this numerical analysis, we can conclude that the eigenmode shows a fascinating behavior with their distortion which correlated with the geometry of the curvature.

Acknowledgements

Author details

Nor Roshidah Yusof, Norshamsuri Ali*, Syed Alwee Aljunid Syed Junid,
Mohd Rashidi Che Beson and Rosdisham Endut
Faculty of Electronic Engineering Technology, Universiti Malaysia Perlis
(UniMAP), Perlis, Malaysia

*Address all correspondence to: norshamsuri@unimap.edu.my

IntechOpen

References

[1] Xavier GB, Lima G. Quantum information processing with space-division multiplexing optical fibres. Communications on Physics. 2020;**3**:9. DOI: 10.1038/s42005-019-0269-7

[2] Agrawal, G. P. (2012). Fiber-optic communication systems (Vol. 222). John Wiley & Sons.

[3] Amnon Yariv, Pochi Yeh (2007). Photonics: Optical Electronics in Modern Communication 6th edition.

[4] Marcuse D. Field deformation and loss caused by curvature of optical fibers. Journal of the Optical Society of America. 1976;**66**:311-320. DOI: 10.1364/JOSA.66.000311

[5] Snitzer E. Cylindrical dielectric waveguide modes*. Journal of the Optical Society of America. 1961;**51**: 491-498. DOI: 10.1364/JOSA.51.000491

[6] Hu J, Menyuk CR. Understanding leaky modes: Slab waveguide revisited. Advances in Optics and Photonics. 2009;**1**:58-106. DOI: 10.1364/AOP.1.000058

[7] P. M. Morse and H. Feshbach, Methods of Theoretical Physics (McGraw-Hill Science/Engineering/Math, 1953).

[8] Marin L, Lesnic D, Mantič V. Treatment of singularities in Helmholtz-type equations using the boundary element method. Journal of Sound and Vibration. 2004;**278**(1–2):39-62. DOI: 10.1016/j.jsv.2003.09.059

[9] Marin L. Treatment of singularities in the method of fundamental solutions for two-dimensional Helmholtz-type equations. Applied Mathematical Modelling. 2010;**34**(6):1615-1633. DOI: 10.1016/j.apm.2009.09.009

[10] Cirone, M. A., Rzążewski, K., Schleich, W. P., Straub, F., & Wheeler, J. A. (2001). Quantum anticentrifugal force. Physical Review A, 65(2), 022101. DOI: 10.1103/PhysRevA.65.022101

[11] Białynicki-Birula I, Cirone MA, Dahl JP, Seligman TH, Straub F, Schleich WP. Quantum fictitious forces. Fortschritte der Physik. 2002;**50**(5–7): 599-607. DOI: 10.1002/1521-3978 (200205)50:5/7<599::AID-PROP599>3.0.CO;2-G

[12] Dandoloff, R., Saxena, A., & Jensen, B. (2010). Geometry-induced potential on a two-dimensional section of a wormhole: Catenoid. Physical Review A, 81(1), 014102. DOI: 10.1103/PhysRevA.81.014102

[13] Dandoloff R, Atanasov V. Quantum anticentrifugal potential in a bent waveguide. Annalen der Physik. 2011; **523**(11):925-930. DOI: 10.1002/andp.201100136

[14] Atanasov, V., & Dandoloff, R. (2015). The curvature of the rotating disk and its quantum manifestation. Physica Scripta, 90, 065001. DOI: 10.1088/0031-8949/90/6/065001

[15] Dandoloff R. Topologically stable states of the anti-centrifugal potential. Journal of Modern Physics. 2019;**10**(08): 1002

[16] M. M. Milosevic, P. S. Matavulj, B. D. Timotijevic, G. T. Reed and G. Z. Mashanovich, "Design Rules for Single-Mode and Polarization-Independent Silicon-on-Insulator Rib Waveguides Using Stress Engineering, " in Journal of Lightwave Technology, vol. 26, no. 13, pp. 1840–1846, July1, 2008, DOI: 10.1109/JLT.2008.922193.

[17] Gajewski A, Gustaw D, Yusof NR, Ali N, Słowik K, Kolenderski P. Waveguide platform for quantum

anticentrifugal force. Optics Letters. 2020;**45**:3373-3376. DOI: 10.1364/ OL.392216

[18] Yusof, N. R., Ali, N., Kolenderski, P., Hambali, N. A., & Aljunid, S. A. (2020, Jan). Geometrical optimization of lithium niobate on insulator rib waveguide for quantum communication application. In AIP Conference Proceedings (Vol. 2203, No. 1, p. 020064). AIP Publishing LLC. DOI: 10.1063/1.5142156